European Journal of Neuroscience, Vol. 9, pp. 113–119, 1997 © European Neuroscience Association

Optical Imaging of Cat Auditory Cortex Cochleotopic Selectivity Evoked by Acute Electrical Stimulation of a Multi-channel Cochlear Implant

Hubert R. Dinse, Ben Godde, Thomas Hilger, Günter Reuter[1], Sven M. Cords[1], Thomas Lenarz[1] and Werner von Seelen
Institut für Neuroinformatik, Theoretische Biologie, Ruhr Universität Bochum, ND 04, D-44780 Bochum, Germany
[1]Medizinische Hochschule Hannover, Experimentelle HNO, D-30623 Hannover, Germany

Keywords: intrinsic signals, receptive fields, representational maps, isofrequency representation, characteristic frequency, cortical plasticity, hearing aids

Abstract

We measured reflectance changes by means of optical imaging of intrinsic signals to study the effects of acute electrical cochlear stimulation on the topography of the cat auditory cortex. After single-pulse electrical stimulation at selected sites of a multichannel implant device, we found topographically restricted response areas representing mainly the high-frequency range in AI. Systematic variation of the stimulation pairs and thus of the cochlear frequency sites revealed a systematic and corresponding shift of the response areas that matched the underlying frequency organization. Intensity functions were usually very steep. Increasingly higher stimulation currents evoked increasingly larger response areas, resulting in decreasing spatial, i.e. cochleotopic, selectivity; however, we observed only slight positional shifts of the focal zones of activity. Electrophysiological recordings of local field potential maps in the same individual animals revealed close correspondence of the locations of the cortical response areas. The results suggest that the method of optical imaging can be used to map response areas evoked by electrical cochlear stimulation, thereby maintaining a profound cochleotopic selectivity. Further experiments in chronically stimulated animals will shed more light on the degree of functional and reorganizational capacities of the primary auditory cortex and could be beneficial for our understanding of the treatment of profound deafness.

Introduction

Cochlear prostheses are increasingly used to provide sound perception in patients with profound deafness of sensorineural origin. By electrical stimulation of the acoustic nerve fibres, their auditory system can be activated in a systematic way that restores to a considerable degree their capacity for hearing. It has been shown that such devices are capable of activating the central auditory pathways over many years. As a consequence of an increasing usage, the question of how they affect the mature central nervous system gains an increasing importance.

Since the introduction of the technique of cochlear implantation (cf. Merzenich and White, 1977), there have been many studies focusing on the investigation of discharge patterns of the auditory nerve fibres after electrical stimulation of the cochlear nucleus or auditory midbrain with an implanted device (Hartmann *et al.*, 1984; Snyder *et al*, 1991; Brown *et al*, 1992). There have been few studies addressing the question of properties of cortical responses after cochlear stimulation (Raggio *et al*, 1992; Raggio and Schreiner, 1994; Fiseifis and Scheich, 1995; Schreiner and Raggio, 1996).

Based on extensive electrophysiological mapping studies using multiple microelectrode penetrations and receptive field measurements, maps of the primary auditory cortex of the cat are characterized by differentially broadly tuned receptive fields, resulting in a fairly strict cochleotopic representation along the caudal–rostral dimension (Merzenich *et al.*, 1975), which is expressed as an increase in the characteristic frequency of neuronal frequency tuning curves (Fig. 1). While the representation of single tones within the framework of cortical maps is fairly well understood (Schreiner, 1991, 1995), little is known about the nature and the degree of the topographic aspects of the representation of cochlear stimulation within cortical maps.

During recent years, new methods have been developed to record optically from the exposed cortex in order to obtain the two-dimensional reflectance changes that have been shown to correspond to the spatial distributions of the underlying neuronal maps (Frostig *et al.*, 1990; Grinvald *et al.*, 1991). These reflectance measurements have the advantage of allowing repeated and multiple measurements of functional maps following sensory stimulation in the same animal, with a spatial resolution of up to 50 μm (Frostig *et al.*, 1990). While the usefulness of this method has been demonstrated in the analysis of the visual (Bonhoeffer and Grinvald, 1991, 1993; Malonek *et al.*, 1994) and more recently also of the somatosensory cortex (Gochin

Correspondence to: Hubert R. Dinse, as above

Received 18 March 1996, revised 29 August 1996, accepted 9 September 1996

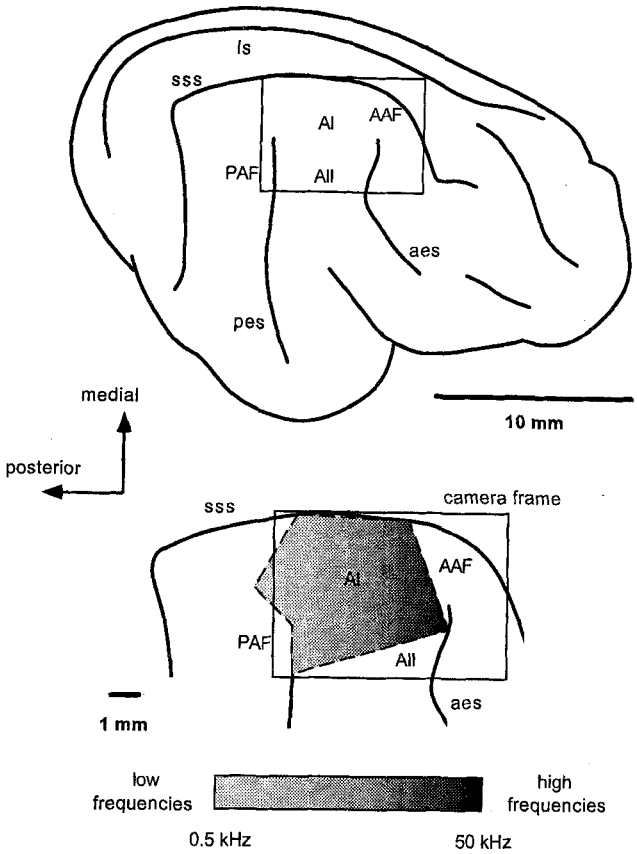

FIG. 1. Top panel shows the layout and parcellation of auditory cortical fields in the cat. AAF, anterior auditory field; AI, primary auditory cortex; AII, secondary auditory field; aes, anterior ectosylvian sulcus; ls, lateral sulcus; PAF, posterior auditory field; pes, posterior ectosylvian sulcus; sss, suprasylvian sulcus. Location of the frame usually used for optical imaging is indicated in the top and bottom panels. At the bottom is an enlarged view together with a schematic drawing of the rostrocaudal frequency gradient. Modified from Imig and Reale (1980).

et al., 1992; Masino *et al.*, 1993; Narayan *et al.*, 1994; Godde *et al.*, 1995a, b), spatially highly resolved maps based on intrinsic signals of the auditory cortex are rare (Hessβ and Scheich, 1995; Bakin *et al.*, 1996), specifically for the auditory cortex of the cat (Dinse *et al.*, 1996). We therefore address the question of the effects of acute electrical cochlear stimulation on the organization of the cochleotopic maps in the auditory cortex of adult cats by means of optical recording of intrinsic signals.

Material and methods

General animal preparation

A total of seven cats were studied. They were anaesthetized for surgery with 25 mg/kg ketamine hydrochloride (Vetalar, Parke Davies) in combination with 1.5 mg/kg xylazine hydrochloride (Rompun, Bayer). Treatment of all animals was according to the US National Institutes of Health Guide for Care and Use of Laboratory Animals (revised 1987). In brief, a craniotomy was performed over the lateral cortex and the dura was removed. All pressure points and wound margins were infiltrated with a local anaesthetic (xylocaine). During the experiment, the animal was continuously infused with 3–9 mg/h of pentobarbital (Nembutal) together with dextrose and electrolytes (Sterofundin, Braun). The body temperature was kept at 37.5–38°C

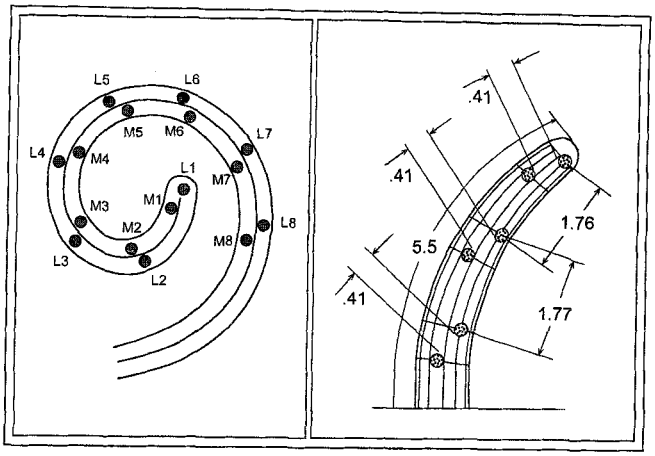

FIG. 2. Schematic illustration of an intracochlear multichannel electrode as used in our cat experiments. Each electrode contained eight bipolar electrode pairs. Electrode 1 was located most distal to the round window. Four of the electrode pairs were inserted via a cochleostomy close to the round window.

and the electrocardiograph was monitored. The animals were acutely deafened by intracochlear injection of neomycin sulphate solution (0.1 ml, 50 mg/ml) in both ears through the round window.

Electrode placement

After a cochleostomy distal to the round window, four pairs of platinum–iridium balls of a human multichannel implant electrode, consisting of a total of eight electrodes, were inserted into the scala tympani. The insertion hole was filled with connective tissue. Inside the bulla tympani bone, the electrode was fixed by glass ionomer cement (Ionos, Seefeld). The other end of the electrode, which contained the galvanic plug connector, was led freely through the skin. A reference electrode was placed under the skin of the occipital bone. The total length of the inserted electrode part was ~8 mm, and the mean distance between electrode sites was ~1.8 mm (Fig. 2). In some cases, the position of the electrode was assessed *post mortem* by roentgenography.

Electrophysiological controls

Conventional electrophysiological controls were made in three cats after the optical imaging session by recording extracellularly action potentials following electrical stimulation of different electrode sites from small clusters of neurons at depths of 600–800 μm using glass microelectrodes (1–2 MΩ) filled with 3 M NaCl. The signals were low-pass filtered to record local field potentials (LFPs) following electrical stimulation of selected electrode positions of the implant device. The spatial distribution of activity (LFP maps) was computed at various levels of LFP amplitude.

Electrical cochlear stimulation

Cochlear stimulation was performed using biphasic current pulses of 75 or 100 μs duration per phase and were delivered via a WPI 365 stimulus isolator. Electrode impedance was checked regularly and was in the range of 5–50 kΩ. Electrical current levels were expressed in dB relative to 100 μA.

Topography of activity

In order to measure the possible underlying topography of activity following cochlear implant electrical stimulation, we stimulated

different pairs of electrode sites with current pulses ~0.5–20 dB above threshold. The different electrode pairs corresponded to different positions in the cochlea and thus to different distances from the round window, resulting in different frequency domains to be stimulated. In some cases, we stimulated selected sites using ground as reference. Six stimuli were applied at a repetition rate of 3 Hz.

Effects of current amplitude

To measure the effect of increasing stimulation current on the topography of the activity distribution, we systematically varied stimulation currents between threshold and 20 dB above threshold.

Electrical auditory brain stem responses

In three animals, electrical auditory brain stem responses (EABRs) were recorded for each electrode pair by means of subdermal steel needle electrodes at the forehead, mastoid and neck (ground). Current amplitude and pulse width (75 μs/phase) were set by a wave generator (Wavetek®, model 175) at a frequency of 30 Hz. Recordings were differentially amplified (×10 000) and band-pass filtered 100 Hz to 1.5 kHz by an analogue–digital converter sampling rate of 25 kHz for a period of 20 ms following stimulus onset (Westra®, model ERA QS/2).

Optical recording

For optical measurements, we used a Lightstar II imaging and acquisition system (LaVision, Gottingen) with a 2 MHz analogue–digital converter and a Peltier-cooled, slow-scan 12 bit digital CCD camera. The CCD was controlled by a 486 PC with 64 MB RAM. Images were obtained with an acquisition time of 80 ms duration. Averaging was achieved by adding intertrial sequences consisting of five images of 80 ms duration, which were averaged to six trials (Godde *et al.*, 1995a, b). Each trial was separated by a pause of 40 s to avoid intertrial interference. The cortex was illuminated with a 546 nm light source. Controls (non-stimulus conditions) were taken as blank images prior to each stimulus presentation. Images were computed by subtracting a stimulus from a non-stimulus condition. Data analysis was performed on Sun workstations using custom-made analysis software written in IDL™. The spatial distributions of reflectance changes were colour-coded and quantitatively computed in terms of cortical area for 25, 50 and 75% of the maximal reflectance changes.

Results

Electrical auditory brain stem responses

In three of the seven animals we measured EABRs prior to optical imaging, using conventional recording techniques. This allowed the assessment of the thresholds of the different electrode pairs and documentation of their effectiveness. We found a latency range of 0.8–1.28 ms for peak II and 2.08–2.80 ms for peak IV. Thresholds were between 100 and 200 μA.

Optical reflectance changes following intracochlear stimulation

We obtained 300 complete optical maps of reflectance changes following different stimulation protocols of the cochlear implant device in seven cats. Each map consisted of a sequence of 12 images of 400 ms duration providing information about the time course of the signals. Accordingly, a total of 3600 single maps were recorded. For further analysis, the frame containing maximal reflectance changes, usually occurring during 2 and 3 s after stimulus onset, was used for further analysis. As a rule, during the temporal development of the optical signal we observed differences in amplitude but not in topography.

Electrical stimulation of radial pairs elicited topographically restricted distributions of optical signals (Fig. 3). On average, the amplitude of the intrinsic signals, i.e. the relative reflectance change measured for the 546 nm light source, was in the range of 0.5–0.8%. The area of the two-dimensional signal distribution increased fairly linearly with signal amplitude. We found an average cortical territory of 0.39 ± 0.32 mm^2 at 75% of the maximal reflectance changes, 2.76 ± 1.91 mm^2 at 50% and 14.73 ± 10.27 mm^2 at 25% (n = 170, maps measured at similar current levels). Generally, the optically obtained distributions of signals were non-homogeneous and often multipeaked, especially in the non-maximal parts of the signals, resulting in complex, patchy patterns of activity.

As can be calculated from the length of the electrode, the position of the stimulation sites and the individual intracochlear position, the frequency range being stimulated was estimated to be between 6 and 50 kHz (see Discussion). According to the position of the implants in the cochlea, response areas in AI were indeed restricted to the high-frequency representations.

Electrophysiological controls: LFP maps

The spatial extent of the underlying neuronal response distributions following single-pulse cochlear electrical stimulation was studied by conventional LFP mappings using up to 40 penetrations in the same animal. These measurements revealed LFP maps of activity distributions that were in remarkable accordance with the spatial reflectance distributions of the optical data imaged in the same animal (Fig. 3A). For this particular recording, we found areas of activation for the 25, 50 and 75% levels of 10.3 versus 10.6 mm^2 (optical imaging versus LFP), 5.6 versus 4.5 mm^2, and 1.8 versus 1.9 mm^2 cortical surface. Comparing all recorded optical imaging and LFP maps (seven maps in three cats) revealed a similar correspondence (9.3 ± 2.89 versus 10.1 ± 2.18; 4.4 ± 1.0 versus 4.5 ± 1.17; 1.1 ± 0.6 versus 1.8 ± 0.46) and was further substantiated by linear regression analysis (r = 0.9537, $P < 0.0001$).

Cochleotopic selectivity

In order to demonstrate that the electrical stimulation of a multichannel cochlear implant preserves cochleotopic selectivity, i.e. evokes response areas that match the underlying frequency-specific organization in AI, we mapped the auditory cortex with intrinsic reflectance measurements for a variety of different stimulation sites.

In the example shown, the reflectance measurements were obtained to electrical stimulation of radial electrode pairs 1–2, 3–4 and 5–8 (Fig. 3C). There was a systematic shift of the response areas towards more anterior sites, which are known to represent successively higher frequencies. There was no overlap between the response areas evoked by stimulating sites 1–2 versus 3–4, and restricted overlap between the stimulation sites 3–4 versus 5–8. In Figure 3Cb, the response areas of each of the three stimulation sites are colour-coded for an amplitude level of 50%, illustrating clear cochleotopic selectivity (combination map). A similar pattern of cochleotopic selectivity was observed when the reference electrode was not one of the implant sites but the general ground. In the example shown in Figure 3B, optical maps for stimulating site 3 versus ground and site 8 versus ground are illustrated.

Effects of intensity of electrical stimulation

Electrical thresholds for generating optical maps were usually in the range of 150–250 μA (3.5–8 dB), but could differ between different

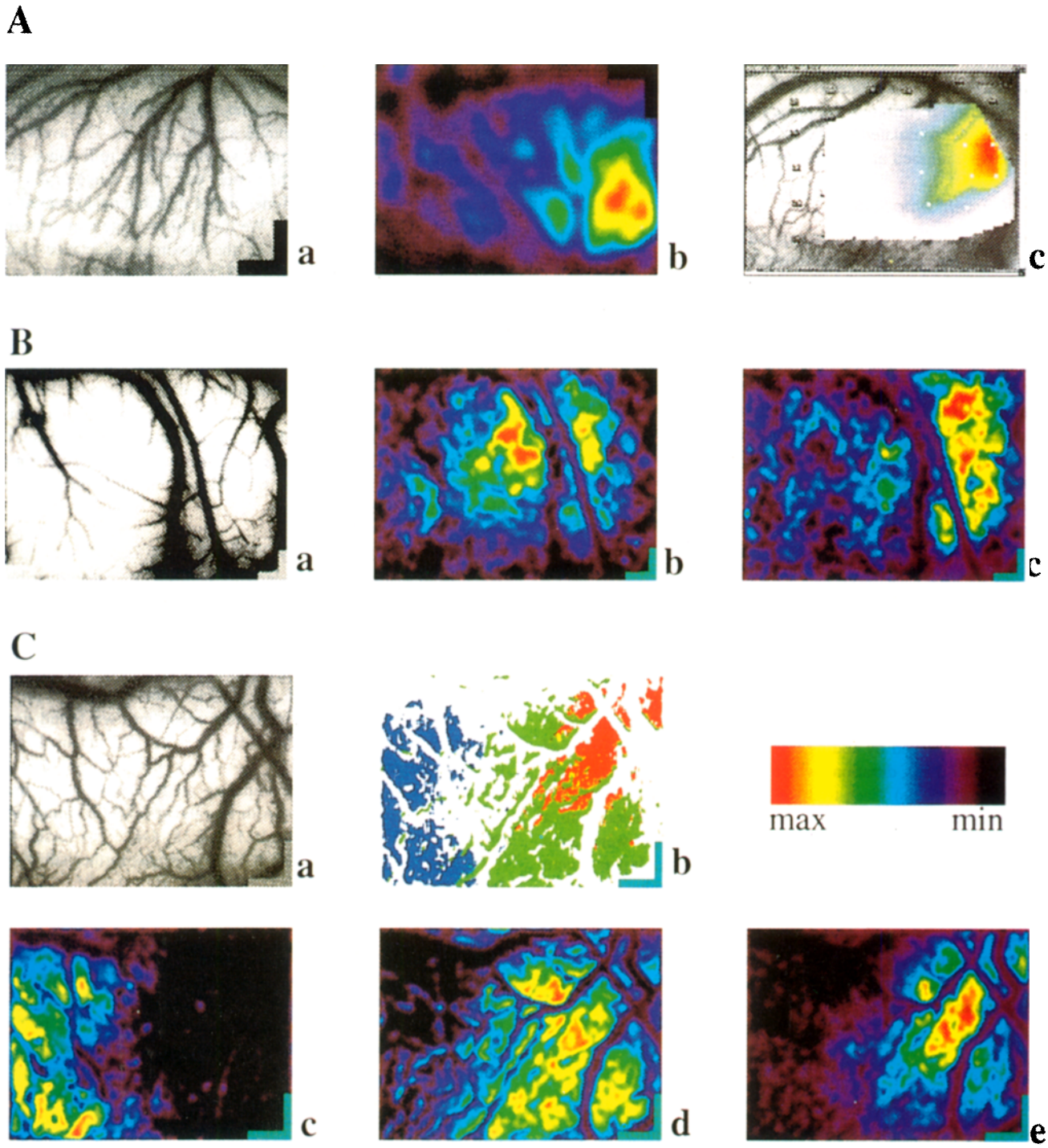

FIG. 3. (A) Comparison of the optically measured spatial reflectance changes of intrinsic signals with the spatial distribution of electrical activity of multiple LFP recordings. Electrical stimulation of electrode positions 1–3 was with 250 μA. Scale bar, 1 mm. (a) Video image of the cortical surface. (b) Topographically restricted reflectance distribution of an optically recorded image following intracochlear stimulation. (c) LFP map superimposed on an image of the cortical surface based on recordings at 35 penetration sites (electrode penetration sites are marked). (B) Cochleotopic selectivity as a result of imaging response maps using two electrode positions that were stimulated with ground as reference. (a) Video image of the cortical surface. (b, c) Map of reflectance changes. (b) Stimulation of electrode 3 versus ground. (c) Stimulation of electrode 8 versus ground. Stimulation current, 12 dB. Scale bar, 1 mm. (C) Cochleotopic selectivity as a result of imaging response maps using three electrode positions. (a) Video image of the cortical surface. (b) Combination map of three different stimulation sites (cf. c–e) obtained for reflectance changes of 50% maximal activity. Blue, electrode pair 1–2; green, electrode pair 3–4; red, electrode pair 5–8. (c–e) Map of reflectance changes. (c) Stimulation of electrode pair 1–2. (d) Stimulation of electrode pair 3–4. (e) Stimulation of electrode pair 5–8. Stimulation current was 15 dB for 1–2 and 3–4, and 18 dB for 5–8. Scale bar, 1 mm.

electrode pairs. Figure 4 shows an example of the effect of increasing stimulation current on the spatial distribution of the evoked optical maps of reflectance changes. The resulting intensity functions were fairly steep. In the example illustrated, a 0.5 dB increase resulted in a two-fold enlargement of the response area. At ~10–15 dB above threshold, a maximal area of excitation was revealed. This enlarge-

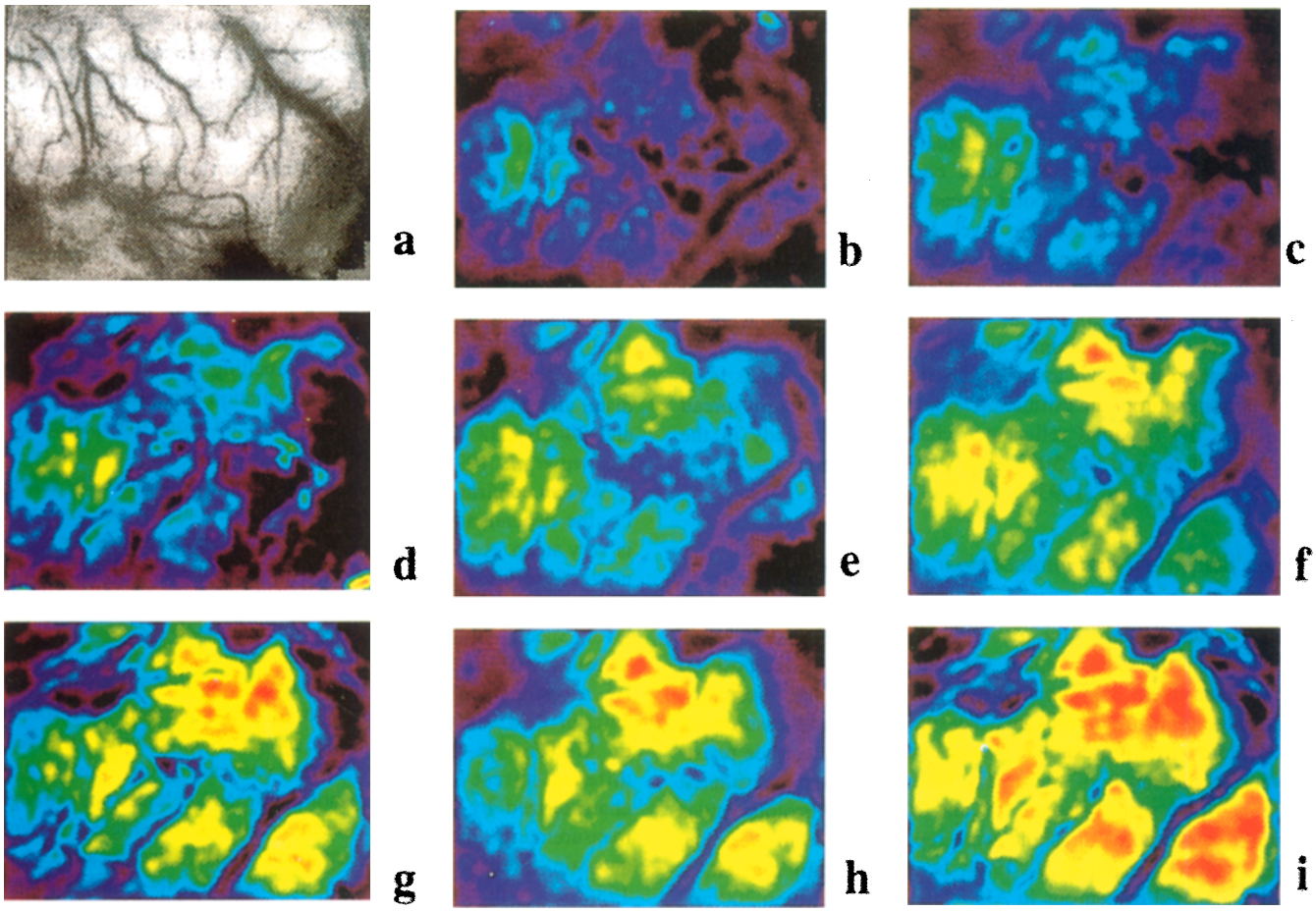

FIG. 4. Effects of increasing stimulation current on the spatial distribution of reflectance changes to stimulation of electrode pair 1–3. Current is indicated as dB relative to 100 μA. (a) Video image of the cortical surface. (b) 3.5 dB. (c) 4.2 dB. (d) 4.5 dB. (e) 4.7 dB. (f) 4.9 dB. (g) 9.5 dB. (h) 14 dB. (i) 17 dB. Scale bar, 1 mm.

ment, parallel to the increase in stimulating current, which was due to increasing recruitment of cortical response areas, reflected the decreasing cochleotopic selectivity of the electrical stimulation. At the same time, during high current stimulation the regions of maximal activity seen during low current stimulation shifted to positions most probably corresponding to auditory fields outside AI (Fig. 4e–f).This enlargement of response areas parallel to the increase of stimulating current reflects a decreasing selectivity of the electrical stimulation. However, there were only slight shifts in the overall position and location of the focal zones of activity emerging during low current stimulation. Instead, the effect of increasing current is mainly reflected in an increasing recruitment of cortical response areas. For example, areas more ventral to AI were sometimes activated, most probably corresponding to AII.

Discussion

The main difference between acoustic and electrical stimulation is that electrically induced activity of the auditory nerve is characterized by high temporal coherence and synchronicity, mainly because no travel times or local mechanical resonance oscillations are involved in their generation. In spite of the methodological differences, we were able to demonstrate that by means of optical recording of intrinsic signals it is possible to image the topographic representation of acute cochlear stimulation in AI and in surrounding auditory cortical fields, and that stimulation of selected locations of a multichannel implant corresponding to different intracochlear frequency locations results in selective shifts of the evoked response areas, which match the underlying frequency organization, and thus preserves the overall cochleotopy.

Advantages of optical imaging of intrinsic signals

There is general agreement about the reliability of optical recording of intrinsic signals, which was demonstrated either by correspondence of optically and electrophysiologically measured representations or by repeated optical measurements revealing low overall variance of the maps together with considerable stability of representational details (Bonhoeffer and Grinvald, 1993). In addition, optical recording of intrinsic signals allows repeated measurements in one animal, which is not possible when the 2-deoxyglucose method is used. This is of considerable importance when parametric studies, which require variation of many parameters, are intended. We were able to measure up to 80 maps in a single animal by systematically varying a large number of stimulus parameters. In addition, we were able to perform a number of repeated measurements, which were used to assess and to demonstrate the reliability of the measured maps. However, in contrast to mapping based on receptive field measurements, optical recording provides measures of the cortical point spread function

(Masino *et al.*, 1993; Grinvald *et al.*, 1994; Godde *et al.*, 1995b; Hilger *et al.*, 1996). Our comparison of optical imaging and LFP data revealed not only a close correspondence between the location and the spatial distribution of the activated area, but also a considerable match concerning the slopes of the activity distributions. Similar results have been found for the rat somatosensory cortex (Hilger *et al.*, 1996). In this study, additional comparison of the optical imaging data with the spiking point spread function revealed a high correlation for the 50% amplitude level. In a study of topographic overlap in the somatosensory cortex of the rat, we found a close match between the estimated width of the cortical point spread function derived from receptive field recordings and the optical signal distribution for the 50% maximal amplitude (Godde *et al.*, 1995b). Based on both results, we assume that the 50% amplitude level provides a more appropriate estimation about the cortical point spread function than the maximal reflectance changes. In a study in the barrel cortex of the rat, the 50% level was also chosen for further analysis by Masino *et al.* (1993).

Electrode placement and intracochlear frequency correspondence

A critical issue concerns the exact location of the stimulating electrodes within the scala tympani. On some occasions, the position could be determined *post mortem* by roentgenography. Normally, controls included electrode resistance measurements and measurement of the absolute current thresholds. Normal values of electrode resistance were in the range of 5–50 kΩ. Thresholds were considered normal when they were between 100 and 200 μA. Absolute values for auditory nerve fibres threshold were reported to be in the range of 60–350 μA (Hartmann *et al.*, 1984; Javel, 1989). In contrast, at the single-cell level of neurons in AI, mean values between 200 and 350 μA have been described, depending on whether radial or longitudinal pairs were stimulated (Raggio and Schreiner, 1994). Moreover, in three animals we measured EABRs. Their latency characteristics, together with appropriate thresholds, provided additional cues for the intactness and proper placement of the electrodes.

We found the most prominent reflectance changes in the high-frequency representation of AI. To provide some absolute values about the frequency ranges stimulated by each electrode, we made use of average data on the length of the scala tympani and their corresponding frequency sites (Schuknecht, 1960; Hatsushika *et al.*, 1990). Based on these data and assuming an overall length of the inserted electrode portion of ~8 mm, we estimate that the frequency range most probably stimulated lay within the range 6–50 kHz. By the same token, assuming a distance of ~2 mm between electrode pairs 1–2, 3–4, 5–6 and 7–8, and assuming that pair 1–2 was located most distal to the round window, frequency differences of 6–12, 12–24 and 24–48 kHz might be expected, i.e. the electrode pairs were presumably separated in the frequency domain by ~1 octave, thus covering a total range of ~3 octaves. However, it must be stated that there was considerable variation from animal to animal, which was probably due to differences in electrode placement. This is reflected in the substantial variation in cortical separation distances, in the range of 1–3 mm of cortical surface for stimulation with different electrode pairs. Optical imaging using tone-burst stimulation in intact cats revealed a mean octave separation of 1–2.5 mm (Dinse *et al.*, 1996), which is in the range to be expected from single-cell mapping (Merzenich *et al.*, 1975). Accordingly, the above calculations based on averaged frequency sites of the scala tympani can only give a rough estimate of the actual electrode positions.

Cochleotopic selectivity and intensity functions

We were able to demonstrate that acute intracochlear stimulation at multiple sites preserves frequency-specific topographies at the level of the auditory cortex. In all cases, electrical stimulation induced patterns of activity that were compatible with known features of the organization of the auditory cortex: patchiness at maximal amplitude levels, spatial orientation in accordance with isofrequency domains at 50% amplitude, and the overall size of activated areas. Earlier studies using only single-site cochlear electrodes were *a priori* not able to address this question. A recent report using conventional electrode mapping provided evidence for the correspondence of functional topographies for acoustic and electrical stimulation (Raggio *et al.*, 1992). Using the method of 2-deoxyglucose labelling performed in the inferior colliculus of the cat, labelling was observed following distal and proximal intracochlear stimulation corresponding to the 12 and 24–26 kHz bands acoustically evoked from the ipsilateral ear (Brown *et al.*, 1992).

We can confirm from our measurements that the intensity function, i.e. the dependency of the signal on the amount of electric current, is very steep. A corresponding finding has been reported for auditory nerve fibres (van den Honert and Stypulkowski, 1987), in which firing rate increases rapidly with only small increases in stimulus level. Specifically during high-current stimulation, we were able to measure widespread reflectance changes in cortical areas surrounding AI, as estimated from the layout of the cortical sulci, such as the anterior field, and more ventral to AI, most probably corresponding to AII (Fig. 4e–f). These shifts in maximal activity, observed at different current levels, suggest that cortical regions outside AI are characterized by higher thresholds. Based on electrophysiological measurements, the high-threshold behaviour of single neurons to acoustic stimulation has been reported for AII (Schreiner and Cynader, 1984). As to the intensity behaviour of AI (Fig. 4b–c), there appeared to be only slight shifts in the overall position and location of the focal zones of activity emerging during low-current stimulation, while at higher currents new zones with even higher levels of activity can evolve outside AI.

Concluding remarks

The rationale behind this study was two-fold. (i) By means of optical imaging techniques the effects of acute electrical stimulation with a multichannel cochlear implant can be visualized. The resulting activity patterns are compatible with known activity maps following acoustic stimulation (Dinse *et al.*, 1996). (ii) The data presented are a necessary baseline for the study of the effects of chronic stimulation in animals with hearing experience and in animals that are neonatally deafened. In view of the well-documented plastic capacities of cortical neurons, widespread reorganizational changes following long-term stimulation might be expected, which in turn might provide the substrate for the highly variable improvement of open speech understanding with practice often observed in patients with such hearing aids (Clark *et al.*, 1987; Reuter *et al.*, 1995). In addition, the way in which cortical systems react to stimulation of cochlear implants can shed light on the principles of cortical information processing strategies, and may therefore be beneficial for our understanding of the specific constraints of auditory processing as well as the development and design of future implants.

Acknowledgements

We gratefully acknowledge the support of the Institut für Neuroinformatik. We thank Drs M. Raggio and C. Schreiner for critical reading of the manuscript. We are grateful to D. Möricke, M. Neef, M. Ziesmer and

W. Dreckmann and the staff of the institute's mechanical shop for excellent technical support. Supported by Deutsche Forschungsgemeinschaft Neurovision Ey 17–3 and BMFT 01VJ 9005.

Abbreviations

AI	primary auditory cortex
AII	secondary auditory field
EABR	electrical auditory brainstem response
LFP	local field potential

References

Bakin, J. S., Kwon, M. C., Masiono, S. A., Weinberger, N. M. and Frostig, R. D. (1996) Suprathreshold auditory cortex activation visualized by intrinsic signal optical imaging. *Cerebral Cortex*, **6**, 120–130.

Bonhoeffer, T. and Grinvald, A. (1991) Iso orientation domains in cat visual cortex are arranged in pinwheel like patterns. *Nature*, **353**, 429–431.

Bonhoeffer, T. and Grinvald, A. (1993) The layout of iso orientation domains in area 18 of cat visual cortex: optical imaging reveals a pinwheel-like organization. *J. Neurosci.*, **13**, 4157–4180.

Brown, M., Shepherd, R. K., Webster, W. R., Martin, R. L. and Clark, G. M. (1992) Cochleotopic selectivity of a multichannel scala tympani electrode array using the 2-deoxyglucose technique. *Hearing Res.*, **59**, 224–240.

Clark, G. M., Blamey, P. J., Brown, A. M., Gusby, P. A., Dowell, R. C., Franz, B. K., Pyman, B. C., Sheperd, R. K., Tong, Y. C. and Webb, R. L. (1987) The University of Melbourne nucleus multi electrode cochlear implant. *Adv. Otorhinolaryngol.*, **38**, 1–181.

Dinse, H. R., Schreiner, C. E., Hilger, T., Godde, B. and von Seelen, W. (1996) Optical imaging of cat auditory cortex functional topographic organization using intrinsic signals. *ARO Midwinter Meeting 1996*, p. 415.

Fiseifis, S. and Scheich, H. (1995) Cochlear prosthesis-induced activity in gerbil's auditory cortex. In Elsner, N. and Menzel, R. (eds), *Learning and Memory*. Thieme, Stuttgart, p. 317.

Frostig, R. D., Lieke, E. E., Ts'o, D. Y. and Grinvald, A. (1990) Cortical functional architecture and local coupling between neuronal activity and the microcirculation revealed by *in vivo* high resolution optical imaging of intrinsic signals. *Proc. Natl Acad. Sci. USA*, **87**, 6082–6086.

Gochin, P. M., Bedenbaugh, P., Gelfand, J. J., Gross, C. G. and Gerstein, G. L. (1992) Intrinsic signal optical imaging in the forepaw area of rat somatosensory cortex. *Proc. Natl Acad. Sci. USA*, **89**, 8381–8383.

Godde, B., Hilger, T., Seelemann, T. and Dinse, H. R. (1995a) Fast mapping of complete cortical representations within minutes. *Soc. Neurosci. Abstr.*, **21**, 119.

Godde, B., Hilger, T., von Seelen, W., Berkefeld, T. and Dinse, H. R. (1995b) Optical imaging of rat somatosensory cortex reveals representational overlap as topographic principle. *NeuroReport*, **7**, 24–28.

Grinvald, A., Frostig, R. D., Siegel, R. M. and Bartfeld, E. (1991) High resolution optical imaging of functional brain architecture in the awake monkey. *Proc. Natl Acad. Sci. USA*, **88**, 11559–11563.

Grinvald, A., Lieke, E., Frostig, R. D. and Hildesheim, R. (1994) Cortical point spread function and long range lateral interactions revealed by real time optical imaging of macaque monkey primary visual cortex. *J. Neurosci.*, **14**, 2545–2568.

Hartmann, R., Topp, G. and Klinke, R. (1984) Discharge pattern of cat primary auditory nerve fibers with electrical stimulation of the cochlea. *Hearing Res.*, **13**, 47–62.

Hatsushika, S. I., Shepherd, R. K., Tong, Y. C., Clark, G. M. and Funasaka, S. (1990) Dimensions of the scala tympani in the human and cat with reference to cochlear implants. *Ann. Otol. Rhinol. Laryngol.*, **99**, 871–876.

Hess, A. and Scheich, H. (1995) Optical recording of intrinsic signals in the auditory cortical fields of the Mongolian gerbil in comparison to 2-DG labeling. In Elsner, N. and Menzel, R. (eds), *Learning and Memory*. Thieme, Stuttgart, p. 306.

Hilger, T., Berkefeld, T., Godde, B., Behrend, K. and Dinse, H. R. (1996) Relation between optical imaging maps and spiking and non-spiking point-spread functions recorded in supragranular and granular laminae in rat somatosensory cortex. *Soc. Neurosci. Abstr.*, **22**, 1057.

Imig, T. J. and Reale, R. A. (1980) Patterns of cortico-cortical connections related to tonotopic maps in cat auditory cortex. *J. Comp. Neurol.*, **192**, 293–332.

Javel, E. (1989) Acoustic and electrical encoding of temporal information. In Miller, J. M. and Spelman, F. A. (eds), *Cochlear Implants—Models of the Electrically Stimulated Ear*. Springer, New York, pp. 247–295.

Malonek, D., Tootell, R. B. H. and Grinvald, A. (1994) Optical imaging reveals the functional architecture of neurons processing shape and motion in owl monkey area MT. *Proc. R. Soc. Lond. Ser. B*, **258**, 109–119.

Masino, S. A., Kwon, M. C., Dory, Y. and Frostig, R. D. (1993) Characterization of functional organization within rat barrel cortex using intrinsic signal optical imaging through a thinned skull. *Proc. Natl Acad. Sci. USA*, **90**, 9998–10002.

Merzenich, M. M., Knight, P. L. and Roth, G. L. (1975) Representation of the cochlea within primary auditory cortex in the cat. *J. Neurophysiol.*, **38**, 231–249.

Merzenich, M. M. and White, M. (1977) Cochlear implant: the interface problem. In Hambrecht, F. T. and Reswick, J. B. (eds), *Functional Electrical Stimulation*. Decker, New York, pp. 321–339.

Narayan, S. M., Santori, E. M. and Toga, A. W. (1994) Mapping functional activity in rodent cortex using optical intrinsic signals. *Cerebral Cortex*, **4**, 195–204.

Raggio, M. W., Schreiner, C. E. and Merzenich, M. M. (1992) Correspondence of functional topographies in cat primary auditory cortex for acoustic and electrical cochlear stimulation. *Soc. Neurosci. Abstr.*, **17**, 382.

Raggio, M. W. and Schreiner, C. E. (1994) Neuronal responses in cat primary auditory cortex to electrical cochlear stimulation. I. Intensity dependence of firing rate and response latency. *J. Neurophysiol.*, **72**, 2334–2359.

Reuter, G., Cords, S. M., Hartrampf, R., Lenarz, T. and Hochmair, I. (1995) Acute effects of high rate stimulation on auditory nerve functions in cats with clinical relevant stimuli. *Conference on Implantable Auditory Prostheses*. Asilomar, USA, p. 47.

Schreiner, C. E. (1991) Functional topographies in the primary auditory cortex of the cat. *Acta Otolaryngol.*, **491**, 7–16.

Schreiner, C. E. (1995) Order and disorder in auditory cortical maps. *Curr. Opin. Neurobiol.*, **5**, 489–496.

Schreiner, C. E. and Cynader, M. S. (1984) Basic functional organization of second auditory cortical field (AII) of the cat. *J. Neurophysiol.*, **51**, 1284–1305.

Schreiner, C. E. and Raggio, M. E. (1996) Neuronal responses in cat primary auditory cortex to electrical cochlear stimulation: II. Repetition rate coding. *J. Neurophysiol.*, **75**, 1283–1300.

Schuknecht, H. F. (1960) Neuroanatomical correlates of auditory sensitivity and pitch discrimination in the cat. In Rasmussen, G. L. and Windle, W. F. (eds), *Neural Mechanisms of the Auditory and Vestibular Systems*. Thomas, Springfield, pp. 76–90.

Snyder, R. L., Rebscher, S. J., Leake, P. A., Kelly, A. and Cao, K. (1991) Chronic intracochlear electrical stimulation in the neonatally deafened ear. II. Temporal properties of neurons in the inferior colliculus. *Hearing Res.*, **56**, 246–264.

van den Honert, C. and Stypulkowski, P. H. (1987) Temporal response patterns of single auditory nerve fibers elicited by periodic electrical stimuli. *Hearing Res.*, **29**, 207–222.